

# The Fabrication by using Surface MEMS of 3C-SiC Micro-heaters and RTD Sensors and their Resultant Properties

Sangsoo Noh\*, Jeonghwan Seo, and Eungahn Lee  
*Research Institute, Daeyang Electric Co., Ltd., Busan 604-030, Republic of Korea*

(Received July 6 2009, Revised August 9 2009, Accepted August 19 2009)

The electrical properties and the microstructure of nitrogen-doped poly 3C-SiC films used for micro thermal sensors were studied according to different thicknesses. Poly 3C-SiC films were deposited by LPCVD (low pressure chemical vapor deposition) at 900°C with a pressure of 4 torr using SiH<sub>2</sub>Cl<sub>2</sub> (100%, 35 sccm) and C<sub>2</sub>H<sub>2</sub> (5% in H<sub>2</sub>, 180 sccm) as the Si and C precursors, and NH<sub>3</sub> (5% in H<sub>2</sub>, 64 sccm) as the dopant source gas. The resistivity of the poly SiC films with a 1,530 Å thickness was 32.7 Ω-cm and decreased to 0.0129 Ω-cm at 16,963 Å. The measurement of the resistance variations at different thicknesses were carried out within the 25°C to 350°C temperature range. While the size of the resistance variation decreased when the films thickness increased, the linearity of the resistance variation improved. Micro heaters and RTD sensors were fabricated on a Si<sub>3</sub>N<sub>4</sub> membrane by using poly 3C-SiC with a 1 μm thickness using a surface MEMS process. The heating temperature of the SiC micro heater, fabricated on 250 μm × 250 μm Si<sub>3</sub>N<sub>4</sub> membrane was 410°C at an 80 mW input power. These 3C-SiC heaters and RTD sensors, fabricated by surface MEMS, have a low power consumption and deliver a good long term stability for the various thermal sensors requiring thermal stability.

**Keywords:** Nitrogen-doped, Poly SiC, LPCVD, Membrane, Micro heater

## 1. INTRODUCTION

The research into micro sensors utilizing micro electromechanical system (MEMS) technology has recently been of great interest[1]. Among these mechanical, chemical and radiant sensors, gas sensors, vacuum sensors and flow sensors are based on the chemical reactions between gas molecules and a sensitive film in order to produce a detectable electrical signal[2,3]. These chemical reactions, such as gas adsorption and desorption, have diffusion effects that significantly depend on the operating temperature, which is an important factor for the optimization of the sensor properties including sensitivity, selectivity and response time. Therefore, micro heaters must be implanted within these sensors to maintain a proper operating temperature. Many measurement and control applications that require micro sensors and micro actuator technologies are used in harsh environments which include exposure to high temperatures, intense vibrations, erosive flows, and/or corrosive media[4]. Silicon carbide (SiC) has an electronic stability at high temperatures, mechanical stiffness, hardness, and chemical inertness, thus making it an exceptional material, since similar devices based on silicon lack the high-temperature capabilities, especially within silicon's electrical and mechanical properties[5]. The development of micro sensors (e.g. micro-heater, thermal flow sensors and chemical sensors) based on the 3C-SiC are very interesting because operating temperatures of more than 400°C can be achieved. Until now, The research into micro heaters (SiC thin films, poly Si, NiFe alloy, NiCr, Pt/Ti and Pt/Cr) using micromachining technology has been actively pursued and these heaters have the following advantages: a low power consumption, an

accurate temperature control, a low heat capacity, and the easy realization of sensor arrays[2,6-10].

In this research, poly SiC was deposited by LPCVD (low pressure chemical vapor deposition) using in-situ nitrogen doping at different thicknesses. The electrical and physical characteristics of the poly SiC thin films were then analyzed by using a four point probe method and by an  $\alpha$ -step method, employing a Scanning Electron Microscope (SEM). A 3C-SiC micro heater was made by a surface MEMS process. The thermal characteristics of the 3C-SiC micro heaters were analyzed by using 3C-SiC Resistance Thermometer Devices (RTDs) integrated on the same substrates; the resistance ratios of the heater and the RTD resistor were also investigated.

## 2. EXPERIMENTS

A conventional, hot-wall, horizontal furnace was used to deposit the nitrogen-doped, 3C-SiC films onto the 100 mm-diameter (100) silicon wafers that were electrically isolated by a thermally-grown SiO<sub>2</sub> layer[11]. The reaction chamber was 2007 mm in length and 225 mm in inner diameter. Poly 3C-SiC films were deposited at 900°C with a pressure of 4 torr, using SiH<sub>2</sub>Cl<sub>2</sub> (100%, 35 sccm) and C<sub>2</sub>H<sub>2</sub> (5% in H<sub>2</sub>, 180 sccm) as the Si and C precursors, and NH<sub>3</sub> (5% in H<sub>2</sub>, 64 sccm) as the dopant source gas. Both the precursor and the dopant gases entered the chamber from the load-end during the film deposition[11]. 3C-SiC films for the micro heaters and the RTD sensors were deposited on a SiO<sub>2</sub>/Si substrate by increasing the thickness from 207 Å to 16,963 Å in order to investigate the electric properties according to thickness.

Figure 1 shows a cross-sectional SEM photo of the 3C-SiC films with a 1 μm thickness used for the testing of the electrical properties. The 3C-SiC films were electrically

\* Author to whom corresponding should be addressed: electronic mail: nss003@daeyang.co.kr

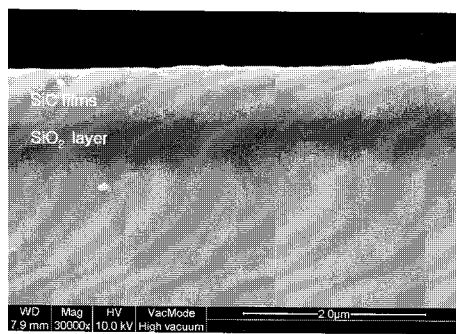


Fig. 1. A SEM micrograph of 3C-SiC film deposited on SiO<sub>2</sub>/Si.

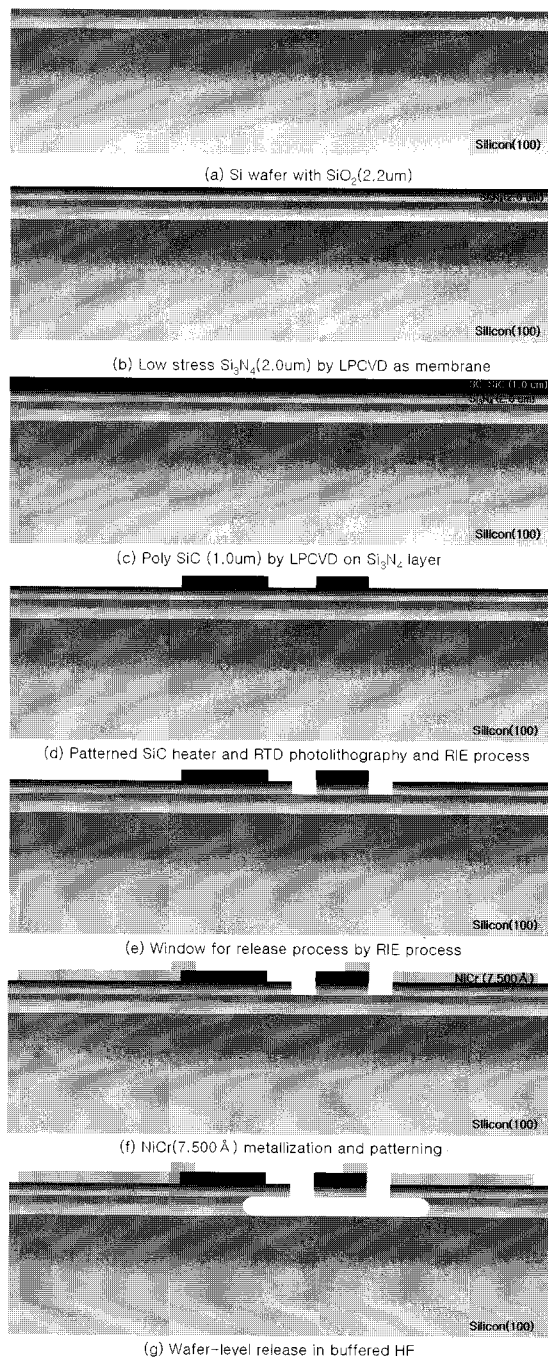


Fig. 2. The fabrication schematic of the 3C-SiC micro heater and the RTD sensors by using a surface MEMS process.

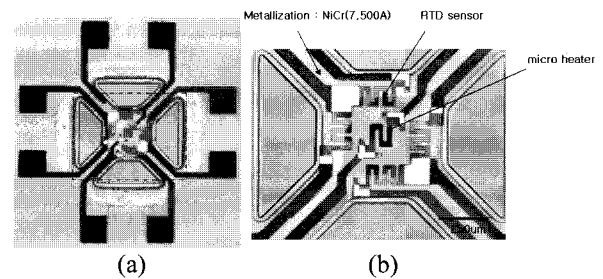


Fig. 3. The 3C-SiC micro heater and the RTD sensors fabricated with a Si<sub>3</sub>N<sub>4</sub> membrane (250 mm × 250 mm) on a Si wafer.

insulated from the Si substrate by the SiO<sub>2</sub> layer so as to remove or reduce the substrate effect during testing at high temperatures[12].

The 3C-SiC micro heaters and the RTD sensors were fabricated by using a surface MEMS process, which is shown in Fig. 2. Figure 3 shows the photographs of a 3C-SiC micro heater and the RTD sensors, which are integrated on the sample substrates.

To minimize the thermal loss through bulk Si, the 3C-SiC micro heater was made on a Si<sub>3</sub>N<sub>4</sub> membrane. The heating property, according to membrane size from 250 μm × 250 μm to 450 μm × 450 μm, was investigated. These properties were analyzed in a closed system, in order to control the atmospheric gas and vacuum conditions, to minimize the convection effects of the atmospheric gas.

The resistances of the poly 3C-SiC films were measured in the 30°C to 450°C operating temperature range by using a hot plate, an accurate multi-meter, a probe station, and a reference temperature sensor. The TCR was then calculated by the following:

$$TCR = \Delta R/R_0 \cdot \Delta T \text{ (ppm/}^\circ\text{C)} \quad (1)$$

where R<sub>0</sub> is the resistance value at 0°C, ΔR is the resistance change with respect to the 0°C resistance, and ΔT is the change in temperature. In order to obtain more accurate data, every measurement was carried out more than ten times, and the average value was then used in each case.

### 3. RESULTS AND A DISCUSSION

Figure 4 represents the resistivity variation as a function of the thickness of 3C-SiC films. In this study, the initial variation of resistivity dropped suddenly as the film's thickness increased, then gradually stabilized as the thickness increased further. The resistivity of poly 3C-SiC films with a thickness of 1,530 Å was 32.7 Ω-cm and decreased to 0.0129 Ω-cm at 16,963 Å.

The surface roughness and grain size according to the film thickness was investigated by using an AFM and a SEM. The grain size of the 3C-SiC films with the thickness of 1,530 Å was 30–40 nm and increased to 350 nm–400 nm at 16,963 Å[13]. Figure 5 shows the results of the AFM analysis (a) and the SEM micrographs (b) of the 3C-SiC films with a 10,155 μm thickness. It shows that the surface morphology of the 3C-SiC films consists of spherical grains. The average surface roughness for each sample was 19–21 nm and the surface grain size was 165 nm–200 nm.

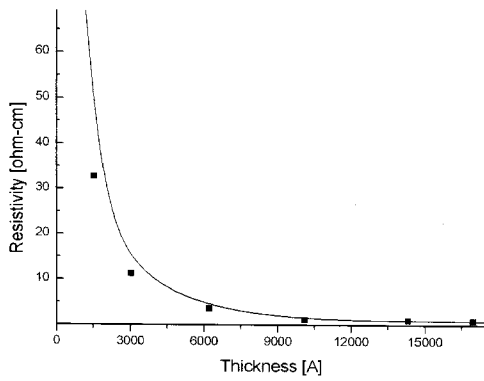


Fig. 4. The resistivity variations of the 3C-SiC films as compared with an increasing thickness.

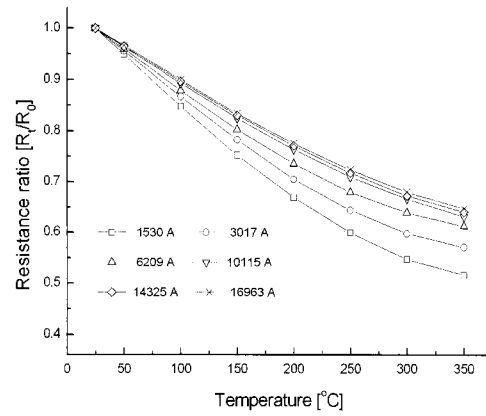


Fig. 6. The resistance ratio of the 3C-SiC films with an increasing temperature.

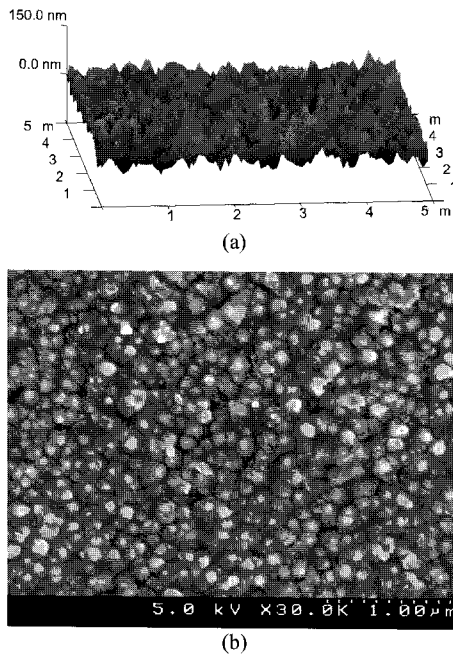


Fig. 5. (a) An AFM micrograph and (b) the surface SEM micrographs of 3C-SiC film at 10,155  $\mu\text{m}$ .

In the application of 3C-SiC films to sensors, the resistance variations of the films were measured. The data is shown in Fig. 6. The grain boundaries in a polycrystalline film lead to electrical properties that are different from the single-crystalline form of the same semiconductor. With an increase in temperature, the thermionic emission of energetic carriers over a potential barrier occurs, resulting in a decrease in the resistivity[14]. A comparison of the variations of 1,530 Å films with 10,115 Å films reveals that the magnitude of the resistance ratio change is much greater in the 1,530 Å films. On the other hand, the linearity of the resistance variation is better in 10,115 Å films. But these variations, according to the film's thickness, are due to a saturation that occurs little by little as the film's thickness increases over 1  $\mu\text{m}$  as shown in Fig. 6.

The TCR value of each sample was measured and its average and standard deviations were calculated in order to understand the distribution of these TCR values. In the case

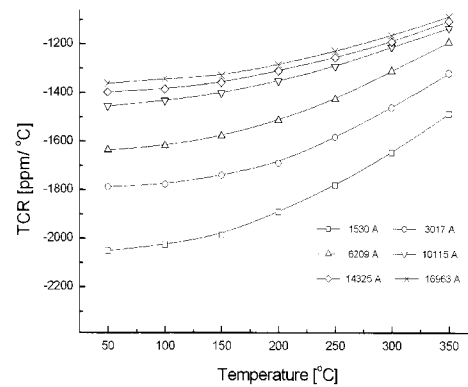


Fig. 7. The TCR variations of 3C-SiC films with different thicknesses.

of 1,530 Å and 10,115 Å, the average TCR was  $-1838.8 \text{ ppm}/^\circ\text{C}$  and  $-1325.9 \text{ ppm}/^\circ\text{C}$ , respectively. In the case of 1,530 Å, the TCR changes from  $-2051.1 \text{ ppm}/^\circ\text{C}$  at  $50^\circ\text{C}$  to  $-1488.1 \text{ ppm}/^\circ\text{C}$  at  $350^\circ\text{C}$ . The TCR standard deviations of 1,530 Å and 10,115 Å were  $517.3 \text{ ppm}/^\circ\text{C}$  and  $292.0 \text{ ppm}/^\circ\text{C}$ , respectively. These facts show that the size of the TCR variation decreases with an increase of the films thickness with an improved linearity.

3C-SiC films with 1  $\mu\text{m}$  of thickness have advantages in both the TCR variation and in linearity. The above results should be considered in the fabrication of micro heaters and RTD sensors. Our fabrication process and the photos of the micro heaters and the RTD sensor were explained in Figs. 1 and 2, respectively. The heating temperature, according to input power, was measured by using RTD sensors located around the 3C-SiC heater. The resistance, measured by a RTD sensor, was calculated and transformed into temperature by using the results of the resistance variation according to temperature. The heating temperature increased due to the differences in thermal loss as the membrane size decreased. This temperature difference became more outstanding with the increase of the input power. The heating temperature of the 3C-SiC micro heater with a  $250 \mu\text{m} \times 250 \mu\text{m}$  membrane size was  $410^\circ\text{C}$  at 80 mW. The heating temperature of the 3C-SiC micro heater with a  $450 \mu\text{m} \times 450 \mu\text{m}$  membrane was  $297^\circ\text{C}$  at 80 mW.

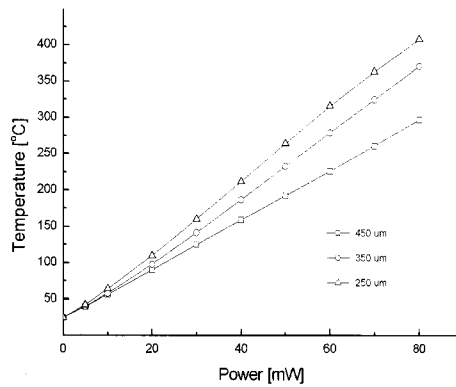


Fig. 8. The heating properties of the 3C-SiC micro heater according to the  $\text{Si}_3\text{N}_4$  membrane size.

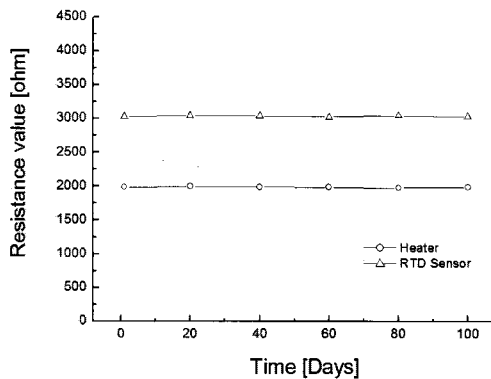


Fig. 9. The resistance variation of the 3C-SiC heater and the RTD after the aging test at 400 °C.

The long term stability of 3C-SiC at a high temperature was tested by heating the fabricated micro heater to 400°C for 100 days. Of course the 3C-SiC RTDs around the heater were tested under the same conditions. The resistance of the 3C-SiC heater and the RTD were 1,900  $\Omega$  and 3,000  $\Omega$ , respectively before the test. Figure 9 shows that these values didn't change after the long term stability test at 400°C for 100 days was completed.

The 3C-SiC heater and the RTD sensor have advantages in their thermal stability and reliability when they are used in an application requiring a long term stability at high temperatures.

#### 4. CONCLUSIONS

The characteristics of 3C-SiC films deposited by LPCVD on a Si substrate coated with  $\text{SiO}_2$  were studied for different

films thickness. The 3C-SiC films were deposited at 900°C and a pressure of 4 torr using  $\text{SiH}_2\text{Cl}_2$  (100%, 35 sccm) and  $\text{C}_2\text{H}_2$  (5% in  $\text{H}_2$ , 180 sccm) as the Si and C precursors, and  $\text{NH}_3$  (5% in  $\text{H}_2$ , 64 sccm) as the dopant source gas. The SiC micro heaters and the RTD sensors were fabricated on a  $\text{Si}_3\text{N}_4$  membrane to minimize the thermal loss through bulk Si by a surface MEMS process.

The resistivity of the 3C-SiC films with the thickness of 1,530 Å was 32.7  $\Omega\text{-cm}$  and decreased to 0.0129  $\Omega\text{-cm}$  at 16,963 Å. The resistance of the nitrogen-doped 3C-SiC films decreased with an increase of the films thickness. The size of the resistance variation decreased, while linearity improved, as the films thickness increased. These properties of the 3C-SiC films, according to the film's thickness, became insensitive over 1  $\mu\text{m}$ . This makes the film's thickness, approximately 1  $\mu\text{m}$ , effective for applications requiring the resistance variations of 3C-SiC films according to temperature changes.

The heating temperature of the 3C-SiC micro heater, fabricated on a 250  $\mu\text{m} \times 250 \mu\text{m}$   $\text{Si}_3\text{N}_4$  membrane was 410°C at an 80 mW input power. These 3C-SiC heaters and RTD sensors, fabricated by surface MEMS, had a low power consumption and delivered a good long term stability for various thermal sensors requiring thermal stability.

#### REFERENCES

- [1] P. M. Sarro, *Sens. Actuators A* **31**, 138 (1992).
- [2] M. A. Gajda and H. Ahmed, *Sens. Actuator A* **49**, 1 (1995).
- [3] L. Qiu, E. Obermeier, and A. Schubert, *Trans. Eurosensors IX*, **130-C2**, 520 (1995).
- [4] M. Mehregany, C. A. Zorman, N. Rajan, and C. H. Wu, *Proceeding of the IEEE*, **86**, 1594 (1998).
- [5] R. Ziermann, J. V. Berg, E. Obermeier, F. Niemann, H. Moller, M. Eickhoff, and G. Krotz, *Conf. Pro. ECSCRM'98, Montpellier, France*, p. 229, (1998).
- [6] V. V. Luchinin, *Tech. Dig. of the 7th Sensor Symp.* p. 30, (1996).
- [7] U. Dibbern, *Sens. Actuator B*, **2**, 63 (1990).
- [8] D. Mutschall, C. Scheibe, and E. Obermeier, *Trans. Eurosensors IX*, **57-PA6**, 256 (1995).
- [9] W. Y. Chung, C. H. Shim, S. D. Choi, and D. D. Lee, *Sens. Actuator B*, **20**, 139 (1994).
- [10] S. H. Lee, I. C. Sub, and Y. K. Sung, *J. Korean Sens. Soc.*, **5**, 69 (1996).
- [11] X. A. Fu, J. L. Dunning, C. A. Zorman, and M. Mehregany, *Sens. Actuator A*, **199**, 169 (2005).
- [12] S. Noh, X. Fu, L. Chen, and M. Mehregany, *Sens. Actuator A*, **136**, 613 (2007).
- [13] S. Noh, J. Seo, and E. Lee, *Trans. Electr. Electron. Mater.* **9**, 101 (2008).
- [14] T. Kamins, *Polycrystalline Silicon for Integrated Circuit Applications*, (Kluwer Academic Publishers, Boston 1988), p. 155.